Available online at www.sciencedirect.com

ScienceDirect

Ceramics International 37 (2011) 2991–2995

CERAMICS INTERNATIONAL

www.elsevier.com/locate/ceramint

The effect of reactor temperature gradient on microstructures of sodium borosilicate glass powders produced by ultrasonic spray pyrolysis technique

Cem Özgür *, Osman Şan

Dumlupinar University, Department of Ceramic Engineering, Kütahya 43100, Turkey

Received 7 February 2011; received in revised form 5 April 2011; accepted 6 April 2011
Available online 13 April 2011

Abstract

Sodium borosilicate glass powders were produced by ultrasonic spray pyrolysis technique for three different reactor temperature gradients and the effect of the reactor temperature gradient on the microstructures of the powders produced was investigated. A three-zone ultrasonic spray pyrolysis system reactor in which the temperatures of each zone could be controlled separately was designed for this purpose. When the drying speed is high, early shell formation was observed in the aerosol droplets due to the difference of the drying speed between inner and outer parts and hollow powders were produced. In order to produce dense powder particles, shell formation on the aerosol droplet should be prevented, therefore drying speed should be decreased. The powders produced were glass-structured, spherical shaped and with smooth surfaces. The density of the hollow powder particle was 1.9 g/cm^3 while the density of the dense particle was 2.5 g/cm^3.

Keywords: A. Powders: chemical preparation; B. Microstructure-final; D. Glass; Hollow glass powder; Spherical powder

1. Introduction

In terms of microstructural control of engineering materials, powders with spherical shape are more advantageous than complex shaped ones. Especially by the production of the porous ceramics, narrow powder particle size is required as well as the spherical shape. Micron-sized spherical powders could be produced with the techniques such as liquid controlled precipitation [1], electron beam evaporation [2], electroprecipitation [3], CVD [4], sol–gel [5], laser ablation [6] and ultrasonic spray pyrolysis [7–19]. Comparing ultrasonic spray pyrolysis technique with the others, it is more advantageous in terms of simplicity and permanence, easy control of the particle size and shape from nano sizes to micro sizes, production of powders with uniform particle size distribution, high purity and obtaining chemical stoichiometry inside the particle [8]. Besides, since powder productions with the other techniques require some special conditions like multiple step procedure and vacuum environment, ultrasonic spray pyrolysis technique is more economical than the others [21].

Ultrasonic spray pyrolysis technique is one of the fundamental techniques used in the last decade for producing micron sized spherical powders and coatings [7,8]. Spherical-shaped oxide [9], non-oxide [10], metal [11], magnetic [12], phosphorus [13], cathode [14], spinel [15], biocompatible [16], super conductive [17], nanocomposite powders [18] were successfully produced with this technique. However, the most unfavorable aspect of this technique is the high possibility of producing hollow particles.

The reason of the hollowness of the particles could be explained as follows. In the system of ultrasonic spray pyrolysis, one single particle is produced from one single aerosol droplet. The aerosol droplet contains water and dissolved or dispersed starting raw materials. When aerosol droplet is exposed to heat, water begins to evaporate. A solid structure forms by the evaporation of water, salts and other components dissolved in water. The fastest evaporation occurs on the surface of the droplet. If there is a small difference between the evaporation speed on the surface and the inner

---

* Corresponding author. Tel.: +90 274 265 20 31/4312; fax: +90 274 265 20 66.
E-mail addresses: cozgur@dumlupinar.edu.tr, cemozgur@ymail.com (C. Özgür).

0272-8842/$36.00 © 2011 Elsevier Ltd and Techna Group S.r.l. All rights reserved.
doi:10.1016/j.ceramint.2011.04.008

parts of the droplet, solid structure occurred equally all through the droplet. Dense particles are produced as such. However, if there is too much difference between the evaporation speeds of the surface and the inner parts, solidification starts immediately and a hard shell occurs on the outer surface of the droplet. Although the outer part of the droplet solidified, inner parts still contained water and since temperature of this water is higher than the evaporation temperature, inclined to diffuse out. If the crust around the droplet is permeable and permits the vapor to go out, water vapor inside diffuses. The particle will be hollow in this case [7].

Generally, two ways are used to produce dense spherical powders with ultrasonic spray pyrolysis technique: to decrease the drying speed of the aerosol droplet using additives or choosing starting raw materials with higher dissolution rate or increasing the dissolution rates of the starting raw materials by additives. Kang et al. produced dense spherical ZrO_2 powders by adding citric acid (CA) and ethylene glycol (EG). In this case, polymeric chains formed depending on the esterification reaction of the carboxyl and hydroxyl groups in citric acid and ethylene glycol. Because of these chains, aerosol droplet turned to a fluid gel in the reactor and volumetric shrinkage could happen, thus dense particles will be produced [20]. In the study of Park et al., drying characteristics of the aerosol droplets changed by changing pH of the solution from which aerosol droplets were obtained of and dense particles produced in this way [22]. Chen et al. reported that the powders produced using starting raw materials with higher dissolution rates were dense. Increasing dissolution rate slowed decrease the shell formation due to recrystallization of the starting raw materials during the evaporation of the water inside the aerosol droplet, thus dense powders were produced [21]. Cho et al. achieved to produce dense powders by increasing dissolution rates of the starting raw materials by adding H_2O_2 to the system [23].

However, using the methods above for producing dense powders with ultrasonic spray pyrolysis technique will cause the costs of the powders to increase and will make the production procedure more complex. In this study, dense powders were obtained by ultrasonic spray pyrolysis technique by control of the reactor temperature gradient. The effect of temperature gradient change on drying speed of the aerosol droplet was investigated and the effect of the temperature gradient on the physical properties, especially density of the powders produced was discussed.

2. Materials and methods

Ultrasonic spray pyrolysis system used for producing of glass powders with spherical shape was given elsewhere in detail [24]. The system can be described into three basic parts as aerosol droplet production, powder formation from aerosol droplets and collection of the powders produced. Production of glass powder using this system was performed as follows: aerosol droplets were produced by ultrasonic nebulizer, these aerosol droplets were fed to the high temperature reactor by the carrier gas, glass powders were produced following evaporation, decomposition and melting reactions within the reactor and the powders were collected. Using this technique, from one aerosol droplet one glass powder particle was obtained. The operating frequency of ultrasonic nebulizer was 1.63 MHz and flow rate of the carrier gas was 2 L/min. The powders produced with ultrasonic spray pyrolysis system were collected by filtration and membranes with a mean pore size of 0.2 μm (Schliecher & Schuell-NL 16).

The schematically description of the reactor used in the study is given in Fig. 1 in detail. In the reactor, a quartz tube with a length of 120 cm and a diameter of 5 cm was used. The lengths of the top zone of the reactor (heating zone 1) and bottom (heating zone 3) were 25 cm each and the length of the middle zone (heating zone 2) was 50 cm. Three different reactor gradients were designed in this study. All reactor zones were operated in the first gradient, bottom and middle reactors were operated for the second gradient, only bottom reactor were operated for the third gradient all at 1200 °C. Temperature inside the reactor was determined with a 100 cm thermocouple wire.

The glass composition was containing 61.22% SiO_2, 17.23% Na_2O, 17.54% B_2O_3 and 4% Al_2O_3 by weight and obtained using Tetraethyl Orthosilicate (TEOS) (Fluka 98%), H_3BO_3

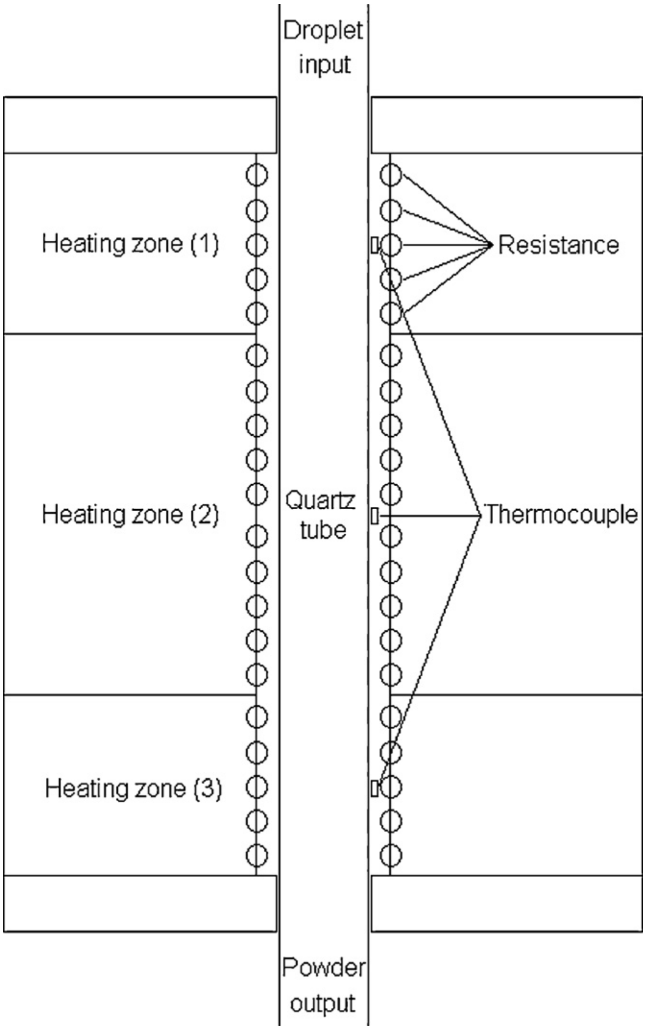

Fig. 1. Schematically description of the reactor used.

(Merck extra pure), $NaNO_3$ (Merck extra pure) and $(Al(NO_3)_3 \cdot 9H_20)$ (Merck). In order to prepare the solution, first TEOS was stirred in water with a magnetic stirrer at 500 rpm until a clear solution was obtained. To obtain a clear solution of TEOS, 0.2 M nitric acid was added. After a clear solution was obtained, other additives (boric acid, sodium nitrate and aluminum nitrate respectively) were added and the solution was stirred with a magnetic stirrer after each addition until a clear solution was formed. The clearness of the solutions was measured with a turbidimeter and when the turbidity value was below 0.1 NTU, solutions were accepted as clear. Solutions were prepared as 2.5 M.

In order to determine the hollowness of the glass powders produced, a glass with the same composition was produced with conventional melting technique and densities of the powders produced with both methods were compared. During the production of glass with classical method, only source of silica was changed and colloidal silica (Merck-extra pure) was used instead of TEOS. The solution prepared from sodium nitrate and boric acid was stirred until a clear solution was obtained and then colloidal silica was added. Then the mix stirred for 30 min at 250 rpm speed for homogeneity. This mixture was dried in an oven at 105 °C for 24 h. Completely dried mixture was homogenized using ball mill at low speed (30 rpm) for 2 h. Then this powder was put into crucibles and melted at 1200 °C for 1 h. At the end of this period, the crucible in the furnace was transferred into a container filled with cold water to cool the melt faster without crystallizing. Glass powder produced using classical melting technique was grinded into a fine sized glass powder with planetary mill for 1 h. Alumina balls were used in planetary mill as grinding material. Solid–liquid ratio in grinding process was 1 by weight.

The phases of the powders produced were determined by XRD (Rigaku-MiniFlex) analysis. XRD analyses were performed at a speed of 2°/min with 0.01° steps using CuKα radiation between 10° and 60°. Particle size distributions were determined with Zetameter (Malvern-Zetameter Nano ZS), specific surface areas with BET (Quantachrome-Nova 2200 e), densities with He-pycnometer (Quantachrome- Ultrapycnometer), morphologies with SEM (Zeiss Supra 50 VP), weight change of the solution due to temperature DTA/TG (Perkin Elmer–Diamond), wall thicknesses of the particles produced with TEM.

3. Results and discussion

The properties of the glass powders produced by ultrasonic spray pyrolysis technique were changing with reactor temperature and temperature gradient. While reactor temperature is mostly effective on the phases of the powders produced, temperature gradient was effective on the shapes of the powders. When the drying speed of the aerosol particle was fast, a shell formed around the aerosol particle and hollow powders were produced. In order to determine the possible shell forming conditions, weight change of the solution with temperature was studied using DTA/TG and results were presented in Fig. 2. There are three zones in the graph with a dramatic weight loss at temperatures between 20 and 130 °C, 130 and 244 °C, and 645 and 730 °C.

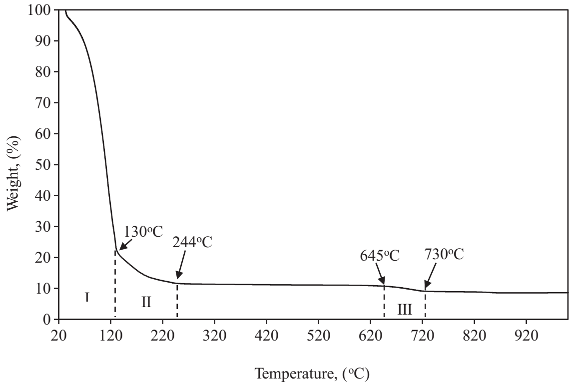

Fig. 2. TG curve of the solution (heating rate = 10 °C/min).

In the first zone, water inside the solution was evaporated. At the end of the first zone (130 °C) total weight loss was 75% approximately. This ratio was so close to total water ratio (74.59% by weight) in the solution which could be accepted as equal. Therefore, all of the water in the solution evaporated in the first zone.

The second zone was decomposition area of TEOS within the aerosol droplet and at the end of this zone; (244 °C) total weight loss was 87.83% approximately. The weight loss would result due to the evaporation of the water inside the aerosol droplet and decomposition of TEOS was 87.78% theoretically. Therefore, evaporation of water and decomposition of TEOS completed at 244 °C. With regard to the physical properties, especially density of the powders produced, the temperature where TEOS started to decompose was important. Hollowness of the particles depended on the possible shell forming temperature rather than reactor temperature [21]. Because of this reason, the shell forming conditions around the aerosol droplet should be determined. Generally, shell formation takes place in two ways: evaporation of water and recrystallization of salts or transformation of liquid phases into solid phases by decomposition as in TEOS. In this study, since TEOS within the aerosol droplet was still in liquid form, even though salts recrystallized due to the evaporation of water when the temperature was lower than 130 °C there was no shell forming around the aerosol droplet. However, shell formation would take place when TEOS would begin to decompose. Therefore, in this study, shell around the aerosol droplet should begin to form when TEOS begins to decompose (130 °C).

The decomposition of the other salts completed at the end of the third zone (730 °C). However, this temperature was higher than the values specified in the literature for decomposition of the salts. The decomposition temperature of boric acid and sodium nitrate is given as 185 °C and 308 °C in the literature, respectively [24]. These decompositions at high temperatures could be explained via the powder production technique where the residence time of the aerosol droplets is very short within the reactor. This phenomenon was discussed in Ref [24] in detail.

Temperature gradients where the powders were produced are shown in Fig. 3. In all three regimes, temperature reached to

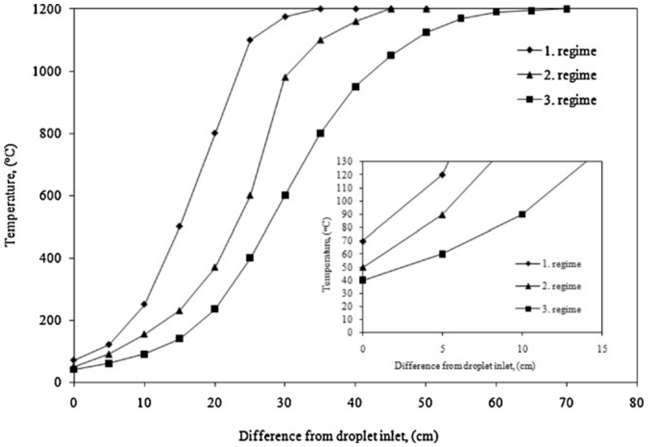

Fig. 3. Reactor temperature gradients.

130 °C, which was the possible shell forming temperature of the aerosol droplet at different distances in the reactor. The distance that the aerosol droplet should cover was 5 cm for the first, 8 cm for the second, and 14 cm for the third regime. Carrier gas speed (2 L/min) was the same for all regimes. Therefore drying speed of the aerosol droplet changed.

Phase analyses of the powders produced by all three regimes are shown in Fig. 4. All of the powders produced had glass structure. Even though the temperature gradient at which the powders were produced changed, maximum reactor temperature (1200 °C) for all three reactors gradient was not changed. However, the powders reached to the maximum temperature at different distances of the reactor. All three regimes, powders cover at least 35 cm at a temperature of 1200 °C. Phase analyses showed that this time span was enough for formation of glass structure (melting).

Microstructures of the same powders are shown in Fig. 5a–c. All powders seem to have spherical shape with smooth surfaces. However, the powders have different mean particle sizes. Mean particle size of the powders are 1346 nm when produced with the first regime, 1302 nm with the second regime and 1227 nm with the last regime. Besides, densities of the powders are also different. While the density of the powders produced with the first regime is 2.05 g/cm^3, 2.23 g/cm^3 with the second regime and 2.49 g/cm^3 with the last regime. The density of the powder produced with classical melting technique is 2.50 g/cm^3. In the light of these, it has been suggested that while the powder produced with the first two regimes were hollow; powders produced with the third regime were dense. The density of the powders produced with the first and the third regimes were studied with TEM and results were shown in Fig. 6a and b. These figures show that while the powder produced with the first regime was hollow with a wall thickness of approximately 200 nm (Fig. 6a); the powder produced with the third regime (Fig. 6b) was dense.

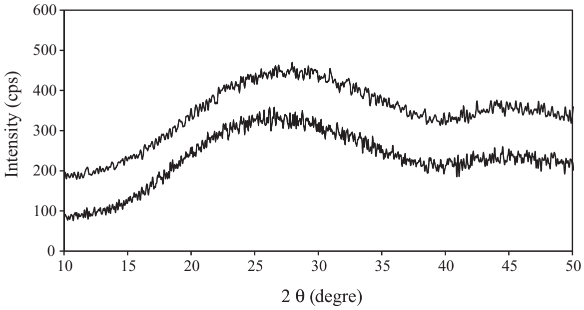

Fig. 4. XRD patterns of the powders prepared with different temperature gradients: regime 1 (bottom), regime 2 (middle) and regime 3 (top).

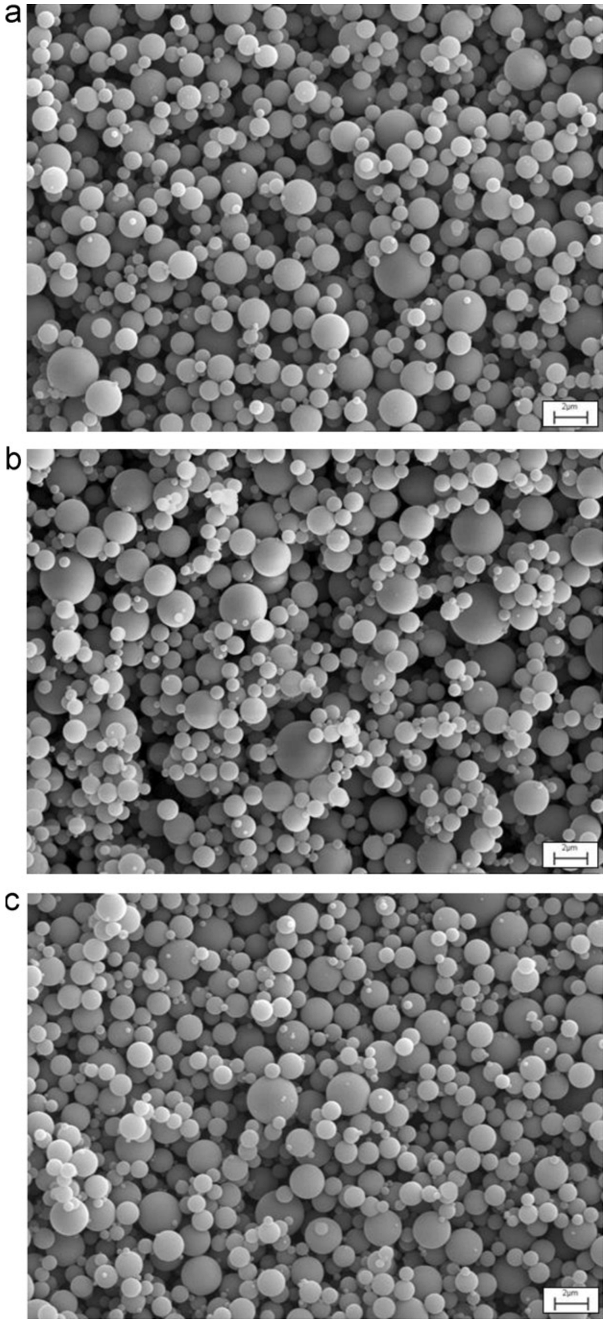

Fig. 5. SEM micrograph of the powder prepared with first regime (a), second regime (b) and third regime (c).

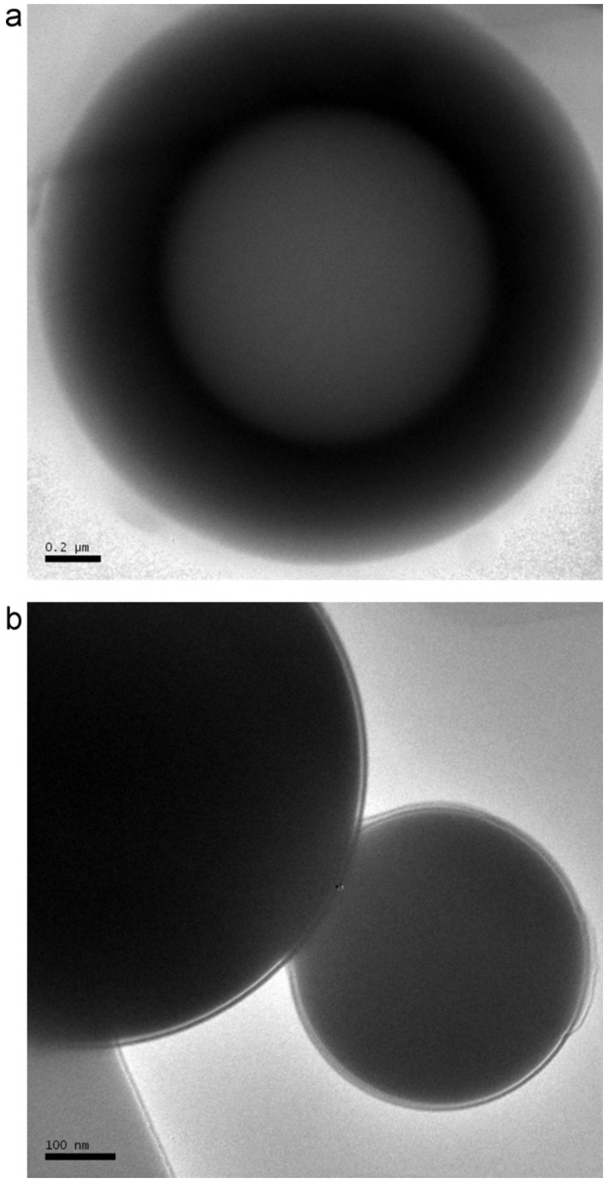

Fig. 6. TEM micrograph of the powder prepared with first regime (a) and third regime (b).

4. Conclusion

In this study sodium borosilicate glass powders were produced using ultrasonic spray pyrolysis technique with three different reactor gradient. The density of the produced glass powders were controlled with shell formation around the outer surface of the aerosol droplets. Shell formation in the production of sodium borosilicate glass powder was controlled with the decomposition of TEOS. In this study, shell formation starting temperature was 130 °C. If aerosol droplet enters fast to this temperature zone, shell formed and powder produced is hollow. However, if it would take a longer time to reach this temperature zone, drying speed of the aerosol droplet decreases. Thus, a dense powder was produced.

References

[1] Y. Li, Y. He, L. Li, Chem. J. Chin. Univ. 20 (1990) 519.
[2] T. Seike, J. Nagaai, Sol. Energy Mater. 22 (1991) 107.
[3] C.N.P. da. Fonseca, M.-A. de. Paoli, A. Gorenstein, Adv. Mater. 3 (1991) 553.
[4] T. Maruyama, S.J. Arai, J. Electrochem. Soc. 143 (1996) 1383.
[5] F. Svegl, B. Orel, I.G. Svegl, V. Kaucic, Electrochim. Acta 45 (2000) 4359.
[6] Y. Wang, Q.-Z. Qin, J. Electrochem. Soc. 149 (2002) 873.
[7] G.L. Messing, S.C. Zhang, G.V. Jayanthi, J. Am. Ceram. Soc. 76 (1993) 2707–2726.
[8] M.M. Bucko, J. Oblakowski, J. Eur. Ceram. Soc. 27 (2007) 3625–3628.
[9] I.Lj. Validzic, V. Jokanovic, D.P. Uskokovic, J.M. Nedeljkovic, J. Eur. Ceram. Soc. 27 (2007) 927–929.
[10] J.H. Kim, V.I. Babushok, T.A. Germer, G.W. Mulholland, S.H. Ehrman, J. Mater. Res. 18 (2003) 1614–1622.
[11] J.-K. Yang, J.-H. Yu, J. Kim, Y.-H. Choa, Mater. Sci. Eng. A 449–451 (2007) 477–479.
[12] E.J. Kim, Y.C. Kang, H.D. Park, S.K. Ryu, Mater. Res. Bull. 38 (2003) 515–524.
[13] T.H. Teng, M.R. Yang, S.H. Wu, Y.P. Chiang, Solid State Commun. 142 (2007) 389–392.
[14] D. Jugovic, N. Cvjeticanin, V. Kusigerski, M. Mitric, M. Miljkovic, D. Makovec, D. Uskokovic, Mater. Res. Bull. 42 (2007) 515–522.
[15] G.-H. An, H.-J. Wang, B.-H. Kim, Y.-G. Jeong, Y.-H. Choa, Mater. Sci. Eng. A 449–451 (2007) 821–824.
[16] A. Kumar, P. Singh, D. Kuar, Cryogenics 46 (2006) 749–758.
[17] Y.C. Kang, S.B. Park, Mater. Lett. 40 (1999) 129–133.
[18] K. Sırakamı, K. Kobayashı, H. Kıkuchı, A. Fuwa, Nippon Kinzoku Gakkaishi 60 (1996) 751–756.
[19] H.Y. Koo, S.K. Hong, S.H. Ju, I.S. Seo, Y.C. Kang, J. Non-Cryst. Solids 352 (2006) 3270–3274.
[20] H.S. Kang, T.C. Kang, H.D. Park, Y.G. Shul, Mater. Lett. 57 (2003) 1288–1294.
[21] C.Y. Chen, T.K. Tseng, S.C. Tsai, C.K. Lin, H.M. Lin, Ceram. Int. 34 (2008) 409–416.
[22] S.-H. Park, S.-W. Oh, S.-T. Myung, Y.C. Kang, Y.-K. Sun, Solid State Ionics. 176 (2005) 481–486.
[23] S.Y. Cho, I.T. Kim, D.Y. Kim, S.J. Park, B.K. Kim, J.H. Lee, Mater. Lett. 32 (1997) 271–273.
[24] C. Özgür, O. Şan, J. Non-Cryst. Solids 356 (2010) 2794–2798.